

Observation of the unidirectional magnetoresistance in antiferromagnetic insulator $\text{Fe}_2\text{O}_3/\text{Pt}$ bilayers

Yihong Fan¹, Pengxiang Zhang², Jiahao Han^{2,s}, Yang Lv¹, Luqiao Liu², and Jian-Ping Wang^{1,*}

¹*Department of Electrical and Computer Engineering, University of Minnesota, 200 Union St. SE, Minneapolis, Minnesota 55455, USA*

²*Department of Electrical Engineering and Computer Science, Massachusetts Institute of Technology, 77 Massachusetts Ave. Room 38-401 Cambridge, MA 02139*

^s*Current address: Research Institute of Electrical Communication, Tohoku University, Sendai 980-8577, Japan*

*Corresponding author: jpwang@umn.edu

Abstract:

Unidirectional magnetoresistance (UMR) has been observed in a variety of stacks with ferromagnetic/spin Hall material bilayer structures. In this work, we reported UMR in antiferromagnetic insulator $\text{Fe}_2\text{O}_3/\text{Pt}$ structure. The UMR has a negative value, which is related to interfacial Rashba coupling and band splitting. Thickness-dependent measurement reveals a potential competition between UMR and the unidirectional spin Hall magnetoresistance (USMR). This work revealed the existence of UMR in antiferromagnetic insulators/heavy metal bilayers and broadens the way for the application of antiferromagnet-based spintronic devices.

The unidirectional spin Hall magnetoresistance (USMR) has attracted a great deal of attention due to its fascinating physics which reveals spin states and electron and magnon transportation properties, as well as application potential in two-terminal reading [1-9]. Compared to the spin Hall magnetoresistance (SMR),

USMR has an angular dependence of 360° rather than 180°, which can reveal the spin-up and spin-down states of the magnetic layer. USMR is first explained with the interfacial spin accumulation and effective current-in-plane giant magnetoresistance [1-3], which is related to the spin Hall effect. Recent research also observed unidirectional magnetoresistive behaviors with different origins, where some of them are spin Hall related and some of them are not. In this case, a more general term of unidirectional magnetoresistance (UMR) is used. Multiple models have been proposed to explain the existence of the UMR and USMR, including spin momentum locking [10,11], magnon contributions [2,12-15], spin-flip contributions [2,13], and spin torque [9].

The spin-orbit torque (SOT) switching of antiferromagnetic material has drawn attention due to its potential in storage applications [16-22]. However, lacking net moment also increases the difficulty to read the switching of the antiferromagnetic order. Conventional reading techniques require 8 or 4 terminals, which significantly increases the complexity and may be debatable because of the thermal-induced magnetoelastic effects [23,37]. Two terminal reading technique is highly demanded in antiferromagnetic spintronics. As the most common two-terminal reading technique, UMR or USMR can be a prospective candidate. However, UMR and USMR have been observed mostly in metallic ferromagnetic systems [1-11] as well as ferromagnetic insulators [15], which reveals their relationship with spin states. Recently, the observation of UMR in antiferromagnetic FeRh/Pt bilayer has paved the way to two-terminal reading in antiferromagnetic systems [24]. Current evidence points out that the potential origin of antiferromagnetic UMR is from interfacial Rashba coupling with the enhancement induced by spin canting [23], which should be confirmed with the existence of UMR or USMR in antiferromagnetic insulator/heavy metal bilayers.

α -Fe₂O₃ is a well-studied antiferromagnetic insulator with room temperature antiferromagnetic phase and strong antiferromagnetic exchange interaction [25,26]. Due to the small net magnetization induced by the Dzyaloshinskii-Moriya (DM) interaction which induces a weak anisotropy [26], a low spin-flop field (<~1T) is observed in α -Fe₂O₃, which provides a platform for current-induced antiferromagnetic switching studies [20-23]. In this work, we observed UMR in antiferromagnetic Fe₂O₃/Pt bilayers. The existence of UMR in

antiferromagnetic insulators provides a way for two-terminal antiferromagnetic reading and indicates an interfacial origin of the UMR signal.

The α -Fe₂O₃ films (60 nm) were grown on α -Al₂O₃ (0001) substrate by magnetron sputtering and post-annealing, which is an easy-plane antiferromagnet according to our previous report ^[23]. The growing methods and film qualities are identical to our previous works ^[22,23,27]. As shown in Figure 1(a), a 120 nm α -Fe₂O₃ was also grown for XRD characterization, and the clear X-ray diffraction (XRD) peak of α -Fe₂O₃ suggests epitaxial growth. The sample was then measured with a SQUID magnetometer at 300 K as shown in Figure 1(b) (easy axis) and 1(c) (hard axis), where a small saturation magnetization of ~ 2 emu/cm³ is observed, as shown in Figure 1(c). Due to the substrate miscut, there is a growth-induced weak uniaxial anisotropy in the easy plane (C-plane), making the three sides of the sample triangle magnetically inequivalent. There is one “easy” side and two other equivalent “hard” sides when we look at the *M*-*H* loops measured along the sides. The “hard” side *M*-*H* loop has a saturation field of 6000 Oe. The Fe₂O₃ observes a saturation field of \sim 6000 Oe at the hard axis [1̄120] and [21̄10] directions. 5 nm Pt was grown on the α -Fe₂O₃ film as a spin Hall channel with magnetron sputtering. The α -Fe₂O₃/Pt stack was then patterned into a Hall bar (Hall channel size \sim 35 μ m \times 10 μ m), with Hall channel direction parallel to the hard axis [21̄10] direction and current flow towards [01̄10] direction, as shown in the left part of Figure 2(a) (see supplementary materials Figure S1 for the sample direction confirmation). The etching removed all the α -Fe₂O₃ film to ensure the absence of nonlocal magnon transport which may influence the measurement ^[27]. However, this long etching may also result in a thinner channel length due to sidewall etching, thus the geometry factors were recharacterized. The patterned device was then measured in a physical property measurement system (PPMS) at 300 K with two SR830 lock-in amplifiers and a Keithley 2182A current source, as shown in the right part of Figure 2(a).

The second harmonic method is used to characterize the UMR and USMR signals ^[1-3,5-9]. A 5 mA AC current with a frequency 133.3 Hz is applied to the device. The first and second harmonic signals are measured with two lock-in amplifiers. The first harmonic signal contains information of SMR (see

supplementary materials Figure S2 for the details of first harmonic signals), and the second harmonic signal contains information of UMR and SOT contributions. The measured second harmonic signals under different magnetic fields are shown in Figure 2(b), where the peak-to-peak signal at 90° and 180° increases with the field. The total signal can be separated into three parts, the contribution of potential UMR, the thermal contribution, and field-like torque contributions. As shown in Figure 2(c) (2(d)), the longitudinal (transverse) angular dependent second harmonic signal is fitted with the following equation ^[15,28]:

$$V_{xx} = \frac{V_{x,SMR} H_{FL}}{2H_{ext}} \sin(2\theta) \cos(\theta) + (V_{x,thermal} + V_{UMR}) \sin(\theta) \quad (1),$$

$$V_{xy} = \frac{V_{y,SMR} H_{FL}}{2H_{ext}} \cos(2\theta) \cos(\theta) + V_{y,thermal} \cos(\theta) \quad (2),$$

where V_{xx} (V_{xy}) is the total measured signal in the longitudinal (transverse) direction, $V_{x,SMR}$ ($V_{y,SMR}$) is the SMR voltage which is related to the contribution of field-like torque, H_{FL} is the field-like torque effective field, H_{ext} is the external field, θ is the angle between current and field, $V_{x,thermal}$ ($V_{y,thermal}$) is the thermal contribution at longitudinal (transverse) direction which includes anomalous Nernst effect (ANE) and spin Seebeck effect (SSE) in the ferromagnetic case ^[1-8] (in the antiferromagnetic case, exclusively SSE), and V_{UMR} is the contribution of UMR, respectively.

To separate $V_{x,thermal}$ from the total signal with $\sin(\theta)$ dependence, the geometry factor needs to be considered. The measured SMR voltage is proportional to the length of the measured area ^[29], which is the length l between the Hall bar channel for the longitudinal case, and the width of the Hall bar w for the transverse case. Meanwhile, the SSE contribution is also proportional to the measured area ^[30], and as a result, there is:

$$\frac{V_{x,SMR}}{V_{y,SMR}} = \frac{V_{x,thermal}}{V_{y,thermal}} \quad (3),$$

with the ratio of the field-like torque induced voltage ($V_{x,SMR}$ and $V_{y,SMR}$), the contribution of thermal effect at longitudinal direction can be calculated with the thermal effect at transverse direction.

Figure 3(a) (3(b)) shows the fitting result of the $\sin(\theta)$ dependent signal for the longitudinal (transverse) measurement at different fields with fitting errors. Both longitudinal and transverse signals have the same linear trend. Figure 3(c) and 3(d)) show the fitting result of the field-like torque term for the longitudinal and transverse measurement under a 30000 Oe magnetic field, respectively. The longitudinal and transverse signals have the same trend, and the signal ratio $\frac{V_{x,SMR}}{V_{y,SMR}}$ is ~ 4.3 , which is slightly larger than the ratio ~ 3.5 in the mask due to sidewall etching and reveals the real geometric ratio of the device. First harmonic SMR signals have given out the similar geometric ratio of the device.

With the geometric ratio, contribution of the UMR signal can be obtained. Figure 4(a) shows the UMR contribution after the removal of the thermal contribution. The resulting UMR have a negative value compared with the thermal effect, which is different from all the other UMR or USMR behaviors observed in ferromagnetic materials. The UMR reaches $\sim 120 \mu\Omega$ with a current of 5 mA, which is 0.00026% per 10^8 A/cm² current density. The value is small compared to the UMR and USMR in ferromagnetic system, but comparable to the UMR in antiferromagnetic systems.

Recent work of UMR in metallic antiferromagnetic stacks [24] has given out a possible explanation to the existence of UMR in α -Fe₂O₃. Existence of interfacial Rashba coupling can produce a nonlinear spin current due to spin-momentum locking and the symmetric distribution of electrons in the momentum space. With an applied magnetic field, the distortion of Fermi contours is significantly increased due to the existence of the spin canting [24], and the level of the distortion is proportional with the applied field, which leads to an observable UMR value. Since both Rashba coupling and band distortion happen at the interface, the existence of UMR in insulator system can be well answered. The negative UMR value may come from the dominance of inner band, which depends on the position of Fermi level and band structure at the interface. Other contributions are also considered. Since a net moment exists in α -Fe₂O₃ and interfacial band splitting can exist at Pt/ferromagnetic interface, as well as the field dependent trend of the UMR signal, it is common to consider the magnetic proximity effect (MPE) as the major contribution. However, previous study of MPE in α -Fe₂O₃ bilayers shows that MPE is not obvious until ultra-low temperature (~ 5 K) [31]. There is no

evidence in antiferromagnet/heavy metal bilayers that the spin canting induced moment can induce MPE in the heavy metal layer. As the UMR increases almost linearly with magnetic field, another explanation may be the bilinear magnetoelectrical resistance (BMER), where the magnetoresistance changes linearly with both magnetic and electrical fields ^[32-34]. However, the control measurement with 5 nm Pt on Al₂O₃ substrate does not observe any signal, suggesting that the α -Fe₂O₃ layer is required for the existence of UMR (see supplementary materials Figure S3 for details).

Recently, an independent report of USMR in α -Fe₂O₃/Pt has also drawn our attention ^[35]. The unidirectional magnetoresistance is observed in the same material system with our observations. The authors conclude the unidirectional magnetoresistance as a USMR behavior induced by thermal random field induced imbalance in magnon creation and annihilation. The USMR value is always positive, and the value first increase then decrease with the field, which seems quite different with our results. Although the magnon creation and annihilation may not be a second order effect generated by the thermal random field considering the large birefringence like magnon transport in α -Fe₂O₃ ^[27], we still consider this explanation a reasonable model. To examine the existence of thermal random field induced magnonic contributions, we measured the UMR value in α -Fe₂O₃(10 nm)/Pt(5 nm) stacks. A thinner magnetic insulator can have better magnon conduction from both top and bottom channels ^[36], which may induce larger magnonic effect contributions. The results are shown in Figure 4(b). At high field, the 10 nm and 60 nm α -Fe₂O₃ samples do not have a significant difference in UMR value, suggesting an interfacial origin of UMR at high field. At low field (<10000 Oe), the net UMR has a positive value. (See supplementary materials Figure S4 for the UMR measurement results of 10 nm and 60 nm samples at low field.) At low field, magnonic USMR may be the dominant term, while at high field, the magnons vanishes and Fermi contour distortion and band splitting become the dominant term for the net UMR signal. A potential competing nature of antiferromagnetic UMR and magnonic USMR is revealed. The origin of antiferromagnet UMR behaviors needs to be explored in the future research.

In conclusion, we have observed a negative unidirectional magnetoresistance in antiferromagnetic α -Fe₂O₃/Pt bilayers with second harmonic measurement. The UMR shows a clear interfacial origin and a negative value, which can be attributed to the Rashba coupling and the Fermi contour distortion under the influence of spin canting. A potential thermal random field induced magnonic USMR is also explored in the α -Fe₂O₃(10 nm)/Pt(5 nm) sample. The UMR presents a signal change from positive to negative for the α -Fe₂O₃(10 nm)/Pt(5 nm) sample, which may reveal a potential competing nature for magnonic USMR and UMR. This work observed UMR in antiferromagnetic insulator and provided evidence of the interfacial origin for UMR in antiferromagnetic materials. This work also paved the way for two-terminal reading in antiferromagnet based spintronic devices.

Note added:

We are aware of an independent report of USMR in α -Fe₂O₃/Pt bilayers ^[35]. The results are developed independently and share many things in common. However, the UMR value in our research is negative and the value increases with field, which is different from that paper. We classified our observations as UMR, and concluded our observations to the interfacial Rashba coupling and band splitting due to the nature of the negative UMR value as reference suggests. However, the results in thinner α -Fe₂O₃ also shows a possibility of magnon and thermal fluctuation induced USMR, which is suggested in the other paper. The commons and conflicts suggest the contribution to UMR or USMR in α -Fe₂O₃ still needs investigation in the future research.

This work was supported, in part, by SMART, one of the seven centers of nCORE, a Semiconductor Research Corporation program, sponsored by the National Institute of Standards and Technology (NIST) and by the UMN MRSEC program under Award No. DMR-2011401. This work utilized the College of Science and Engineering (CSE) Characterization Facility at the University of Minnesota (UMN) supported,

in part, by the NSF through the UMN MRSEC program. Portions of this work were conducted in the Minnesota Nano Center, which is supported by the National Science Foundation through the National Nano Coordinated Infrastructure Network (NNCI) under Award Number ECCS-2025124. P. Z. acknowledges support from Mathworks fellowship. J.-P.W. also acknowledges support from Robert Hartmann Endowed Chair Professorship.

The data that support the findings of this study are available from the corresponding author upon reasonable request.

Reference:

- [1] Avci, Can Onur, et al. "Unidirectional spin Hall magnetoresistance in ferromagnet/normal metal bilayers." *Nature Physics* 11.7 (2015): 570-575.
- [2] Avci, Can Onur, Kevin Garello, Abhijit Ghosh, et al. "Origins of the unidirectional spin Hall magnetoresistance in metallic bilayers." *Physical review letters* 121.8 (2018): 087207.
- [3] Zhang, Steven S-L., and Giovanni Vignale. "Theory of unidirectional spin Hall magnetoresistance in heavy-metal/ferromagnetic-metal bilayers." *Physical Review B* 94.14 (2016): 140411.
- [4] Duy Khang, Nguyen Huynh, and Pham Nam Hai. "Giant unidirectional spin Hall magnetoresistance in topological insulator–ferromagnetic semiconductor heterostructures." *Journal of Applied Physics* 126.23 (2019): 233903.
- [5] Sterk, W. P., D. Peerlings, and R. A. Duine. "Magnon contribution to unidirectional spin Hall magnetoresistance in ferromagnetic-insulator/heavy-metal bilayers." *Physical Review B* 99.6 (2019): 064438.
- [6] Lv, Yang, James Kally, Delin Zhang, et al. "Unidirectional spin-Hall and Rashba– Edelstein magnetoresistance in topological insulator-ferromagnet layer heterostructures." *Nature communications* 9.1 (2018): 1-7.

[7] Lv, Yang, James Kally, Tao Liu, et al. "Large unidirectional spin Hall and Rashba– Edelstein magnetoresistance in topological insulator/magnetic insulator heterostructures." *Applied Physics Reviews* 9.1 (2022): 011406.

[8] Fan, Yihong, et al. "Observation of unidirectional spin Hall magnetoresistance in amorphous PtSn₄/CoFeB bilayers." *Applied Physics Letters* 121.9 (2022): 092401.

[9] Chang, Ting-Yu, et al. "Large unidirectional magnetoresistance in metallic heterostructures in the spin transfer torque regime." *Physical Review B* 104.2 (2021): 024432.

[10] Yasuda, Kenji, et al. "Large unidirectional magnetoresistance in a magnetic topological insulator." *Physical review letters* 117.12 (2016): 127202.

[11] Guillet, T., et al. "Observation of large unidirectional Rashba magnetoresistance in Ge (111)." *Physical Review Letters* 124.2 (2020): 027201.

[12] Sterk, W. P., D. Peerlings, and R. A. Duine. "Magnon contribution to unidirectional spin Hall magnetoresistance in ferromagnetic-insulator/heavy-metal bilayers." *Physical Review B* 99.6 (2019): 064438.

[13] Kim, Kab-Jin, et al. "Possible contribution of high-energy magnons to unidirectional magnetoresistance in metallic bilayers." *Applied Physics Express* 12.6 (2019): 063001.

[14] Nguyen, Thanh Huong Thi, et al. "Unidirectional spin Hall magnetoresistance in epitaxial Cr/Fe bilayer from electron-magnon scattering." *Communications Physics* 4.1 (2021): 1-8.

[15] Liu, G., et al. "Magnonic Unidirectional Spin Hall Magnetoresistance in a Heavy-Metal–Ferromagnetic-Insulator Bilayer." *Physical Review Letters* 127.20 (2021): 207206.

[16] Fukami, Shunsuke, et al. "Magnetization switching by spin–orbit torque in an antiferromagnet–ferromagnet bilayer system." *Nature materials* 15.5 (2016): 535-541.

[17] Chen, Xianzhe, et al. "Electric field control of Néel spin–orbit torque in an antiferromagnet." *Nature materials* 18.9 (2019): 931-935.

[18] Zhou, X. F., et al. "Strong orientation-dependent spin-orbit torque in thin films of the antiferromagnet Mn 2 Au." *Physical Review Applied* 9.5 (2018): 054028.

[19] Yan, Z., et al. "Current switching of interface antiferromagnet in ferromagnet/antiferromagnet heterostructure." *Applied Physics Letters* 118.3 (2021): 032402.

[20] Huang, Lin, et al. "Terahertz pulse-induced Néel vector switching in α -Fe2O3/Pt heterostructures." *Applied Physics Letters* 119.21 (2021): 212401.

[21] Cheng, Yang, et al. "Electrical Switching of Tristate Antiferromagnetic Néel Order in α -Fe2O3 Epitaxial Films." *Physical Review Letters* 124.2 (2020): 027202.

[22] Wang, Hailong, et al. "Spin-orbit-torque switching mediated by an antiferromagnetic insulator." *Physical Review Applied* 11.4 (2019): 044070.

[23] Zhang, Pengxiang, et al. "Quantitative study on current-induced effect in an antiferromagnet insulator/Pt bilayer film." *Physical Review Letters* 123.24 (2019): 247206.

[24] Shim, Soho, et al. "Unidirectional Magnetoresistance in Antiferromagnet/Heavy-Metal Bilayers." *Physical Review X* 12.2 (2022): 021069.

[25] Elliston, P. R., and G. J. Troup. "Some antiferromagnetic resonance measurements in α -Fe2O3." *Journal of Physics C: Solid State Physics* 1.1 (1968): 169.

[26] Williamson, Samuel J., and Simon Foner. "Antiferromagnetic Resonance in Systems with Dzyaloshinsky-Moriya Coupling; Orientation Dependence in α Fe2O3." *Physical Review* 136.4A (1964): A1102.

[27] Han, Jiahao, et al. "Birefringence-like spin transport via linearly polarized antiferromagnetic magnons." *Nature nanotechnology* 15.7 (2020): 563-568.

[28] Cheng, Yang, et al. "Third harmonic characterization of antiferromagnetic heterostructures." *Nature communications* 13.1 (2022): 1-6.

[29] Chen, Yan-Ting, et al. "Theory of spin Hall magnetoresistance." *Physical Review B* 87.14 (2013): 144411.

[30] Uchida, K., et al. "Observation of the spin Seebeck effect." *Nature* 455.7214 (2008): 778-781.

[31] Cheng, Yang, et al. "Anisotropic magnetoresistance and nontrivial spin Hall magnetoresistance in Pt/ α -Fe 2 O 3 bilayers." *Physical Review B* 100.22 (2019): 220408.

[32] He, Pan, et al. "Bilinear magnetoelectric resistance as a probe of three-dimensional spin texture in topological surface states." *Nature Physics* 14.5 (2018): 495-499.

[33] Zhang, Yuejie, et al. "Large magnetoelectric resistance in the topological Dirac semimetal α -Sn." *Science advances* 8.30 (2022): eab0052.

[34] Zhang, Steven S-L., and Giovanni Vignale. "Theory of bilinear magneto-electric resistance from topological-insulator surface states." *Spintronics XI*. Vol. 10732. SPIE, 2018.

[35] Cheng, Yang, et al. "Unidirectional Spin Hall Magnetoresistance in Antiferromagnetic Heterostructures." *arXiv preprint arXiv:2207.10346* (2022).

[36] Zhou, X. J., et al. "Lateral transport properties of thermally excited magnons in yttrium iron garnet films." *Applied Physics Letters* 110.6 (2017): 062407.

[37] Sheng, Peng, et al. "Thermal contribution in the electrical switching experiments with heavy metal/antiferromagnet structures." *Journal of Applied Physics* 132.7 (2022): 073902.

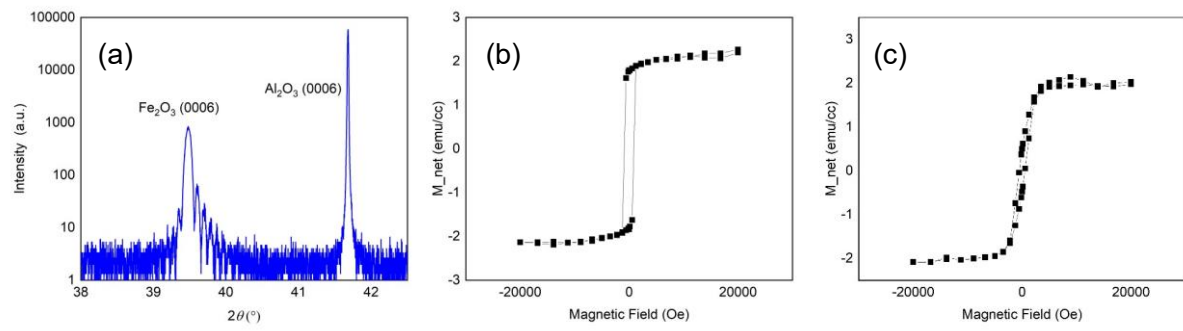


Figure 1. (a) The X-ray diffraction pattern for α - Fe_2O_3 (120 nm) sample. The SQUID measurement of easy axis $[\bar{1}2\bar{1}0]$ and hard axis $[2\bar{1}\bar{1}0]$ is shown in Figure 1(b) and 1(c) respectively,

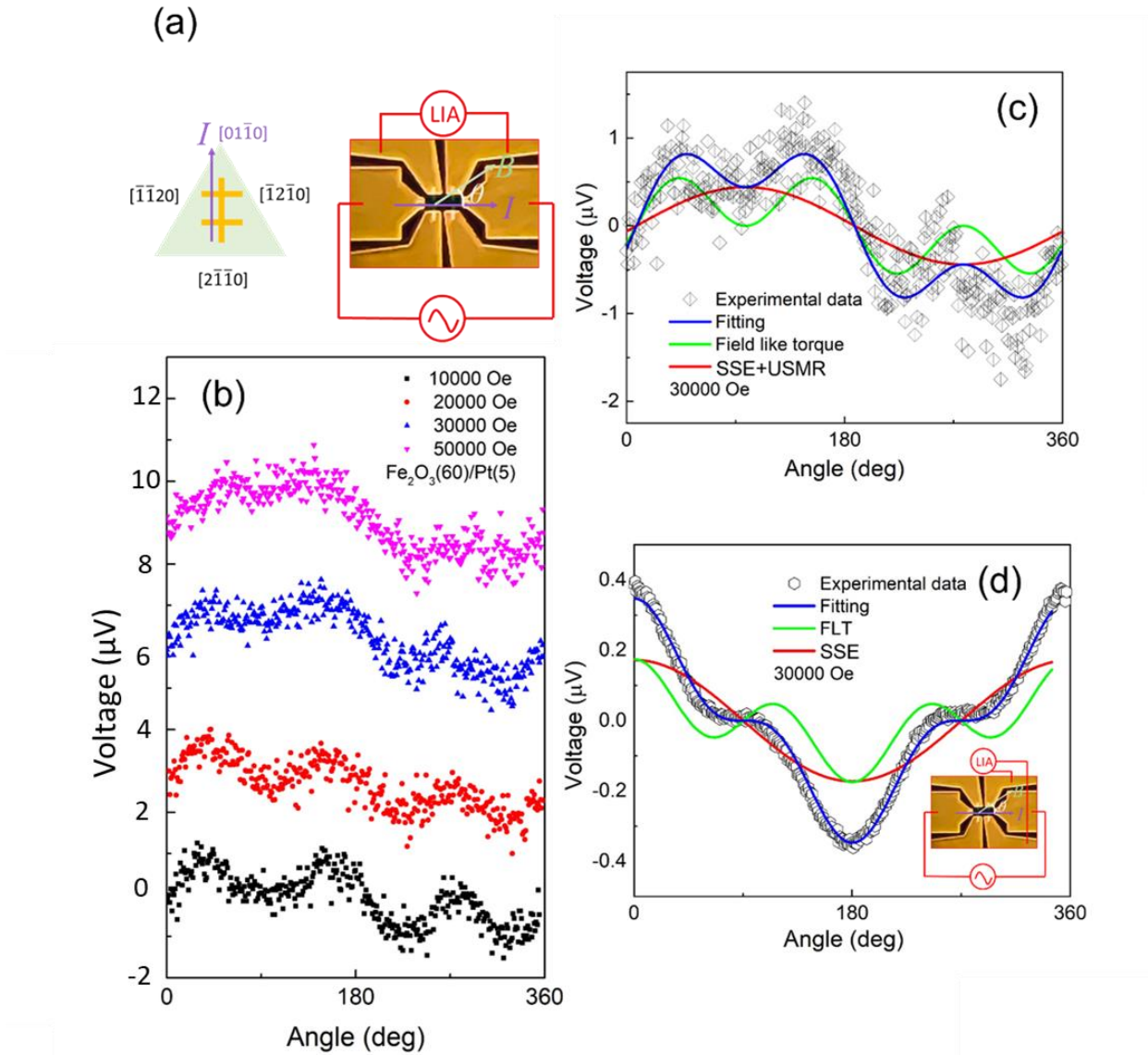


Figure 2. (a) The left section is an illustration of the sample patterning position respect to the sample crystalline direction. The right section is an illustration of the longitudinal second harmonic measurement. LIA stands for lock-in amplifier. (b) Measured longitudinal second harmonic signals under different fields. (c) Fitting of the longitudinal second harmonic signal. (d) Fitting of the transverse second harmonic signal. The transverse measurement illustration is shown in the inner part of the figure.

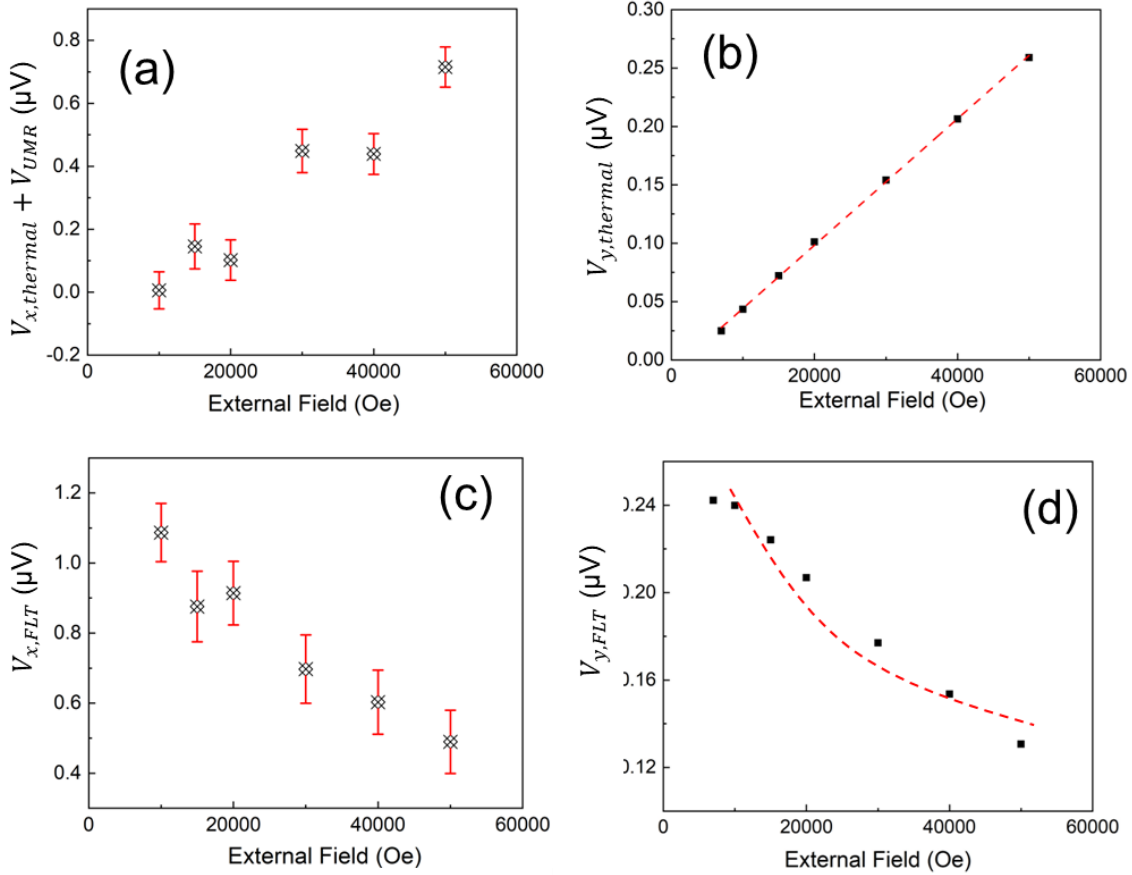


Figure 3. (a) Field dependence of the longitudinal 360° dependent voltage $V_{x,thermal} + V_{UMR}$. (b) Field dependence of the transverse 360° dependent voltage $V_{y,thermal}$, which is almost proportional to the external field. (c) Field dependence of the longitudinal field-like torque voltage $V_{x,FLT} = \frac{V_{x,SMR}H_{FL}}{2H_{ext}}$. (d) Field dependence of the transverse field-like torque voltage $V_{y,FLT} = \frac{V_{y,SMR}H_{FL}}{2H_{ext}}$.

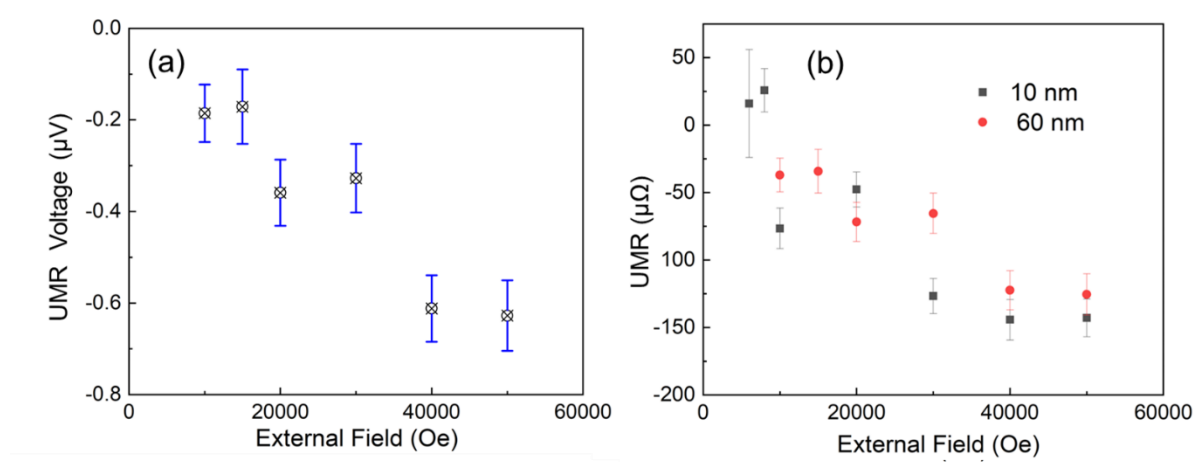


Figure 4. (a) Observed net UMR voltage in $\alpha\text{-Fe}_2\text{O}_3(60 \text{ nm})/\text{Pt}(5 \text{ nm})$ sample. The UMR has a negative value. (b) Observed net UMR value in $\alpha\text{-Fe}_2\text{O}_3(60 \text{ nm})/\text{Pt}(5 \text{ nm})$ and $\alpha\text{-Fe}_2\text{O}_3(10 \text{ nm})/\text{Pt}(5 \text{ nm})$ stacks. The UMR in $\alpha\text{-Fe}_2\text{O}_3(10 \text{ nm})/\text{Pt}(5 \text{ nm})$ observed a signal change at ~ 10000 Oe, suggesting a competing scheme of magnonic and Rashba SOC origins.